STRUCTURAL INTEGRITY ASSESSMENT OF SPHERICAL STORAGE TANKS

Gorgi Adžiev (1), Aleksandar Sedmak (2), Todor Adžiev (1), Stojan Sedmak (3)
(1) Faculty of Mechanical Engineering, University of Skopje, Macedonia
(2) Faculty of Mechanical Engineering, University of Belgrade, Serbia and Montenegro
(3) Faculty of Technology and Metallurgy, University of Belgrade, Serbia and Montenegro
(2) aleksandar_sedmak@mntr.sr.gov.yu
(3) asedmak@eunet.yu

Abstract

Two spherical storage tanks for ammonia (volume 1000 m^3) have been tested in 1998 and 1999 by Non-Destructive Techniques (NDT) in accordance with the Periodic Inspection Regulations. These storage tanks have been constructed in 1979 using microalloyed steel St.E460 according to DIN, with thickness of 30 mm. The large number of transverse cracks in weld metal and longitudinal cracks in heat-affected-zone and along fusion line of inner welded joints has been detected. In order to estimate the residual strength, from both storage tanks, plates 500x500 mm were cut for the chemical, metallurgical and mechanical investigations. These investigations encompassed detailed toughness testing, including standard Charpy specimens, tested on instrumented pendulum, and fracture mechanics testing on standard SENB specimens for fracture toughness evaluation. Using data obtained by Charpy and fracture mechanics testing, the structral integrity of cracked storage tanks has been assessed.

Key words:

Spherical Storage Tank, Structural Integrity, Strength Mismatching, Crack Driving Force, J Resistance Curve

Introduction

Two spherical storage tanks for ammonia (volume 1000 m^3, diameter D=12400 mm and thickness t=30 mm, Fig. 1), with the maximum operating pressure p=16.5 bar and the test pressure for periodical inspections p = 25 bar, have been tested in 1998 and 1999 by Non-Destructive Techniques (NDT) in accordance with the Periodic Inspection Regulations. The storage tanks have been constructed in 1979 using microalloyed steel St.E460 according to DIN, with nominal yield strength $R_{p0.2}$ = 460 MPa. The chemical analysis is given in Table 1. Tensile properties, obtained in tensile tests, are presented in Table 2 as an average of several test results.

Table 1. Chemical analysis, %

C	Si	Mn	P	S	Ti	Cr	Al	Cu	Ni	V	Mo	Nb
0.2	0.44	1.35	0.012	0.01	0.12	0.15	0.06	0.05	0.1	0.008	0.015	0.001

Table 2. Tensile properties

Yield strength	Tensile strength	Elongation
$R_{p0.2}$ (MPa)	R_m (MPa)	A_5 (%)
420	604	25

For NDT ultrasonics, dye penetrant and magnetic particle technique have been used. The last one, in combination with fluorescent light, turned out to be the most efficient for detection of surface and small subsurface cracks. A large number of transverse cracks in weld metal and longitudinal cracks in heat-affected-zone (HAZ) along fusion line of inner welded joints has been detected, like one shown in Fig. 2. The longitudinal cracks were considered as more dangerous due to their size (length up to 300 mm, depth up to 12 mm) and position.

FIGURE 1. Spherical storage tanks

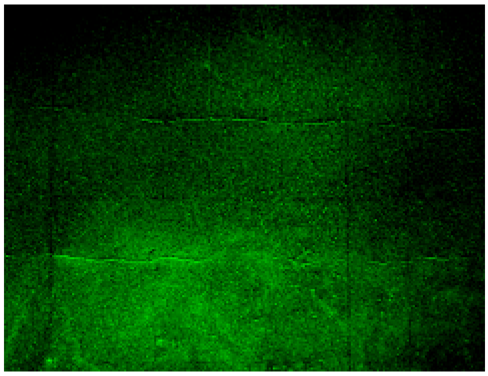

FIGURE 2. Cracks along fusion line

Cracks were removed by grinding out the crack up to its bottom (tip) and surrounding area. After this the original dimensions were recovered by subsequent surface welding, using the welding procedure, as shown in [1]. Anyhow, having in mind possibility of overlooking another crack it was decided to perform detailed experimental and numerical analysis of fracture behaviour of weldments in order to assess completely the structural integrity of storage tanks.

Experimental investigation and results

Tensile specimens (width *W*=24 mm, thickness *B*=20 mm, length *L*=300 mm, Fig. 3) were machined out of the spare trial welded plate (400 x 400 mm), as shown in Fig. 4. In the scope of this investigation other mechanical tests (e.g. instrumented Charpy test) were performed, as described in [1].

Cracks were produced by electro-erosion because by standard fatigue procedure it was practically impossible to locate the crack tip in very narrow HAZ subregions (fine grain – FGHAZ and coarse grain - CGHAZ). A special procedure was applied, including very small amperage (cca 1 A) in order to get crack tip as sharp as possible (below 0.05 mm, as shown schematically in Fig. 5).

Specimens were designed in a way to simulate real conditions as a simplified model, since significant length (~300 mm) of the detected longitudinal cracks makes the effect of first principal stress dominant by crack opening and thus the effect of the second principal stress negligible.

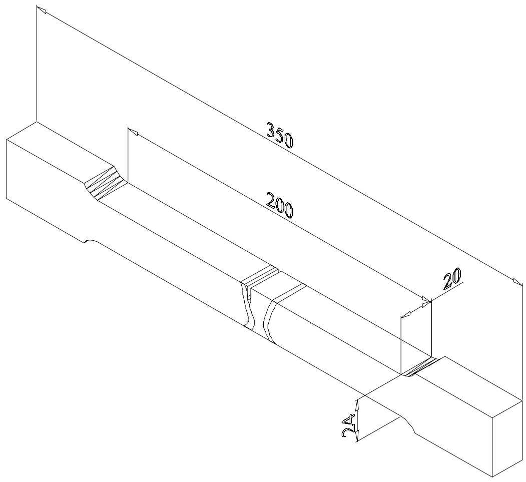

FIGURE 3. Specimen isometric view

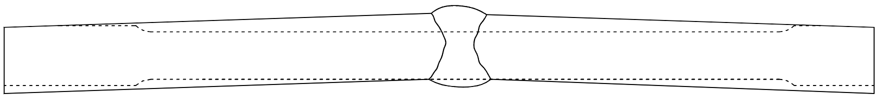

FIGURE 4. Extraction of a specimen

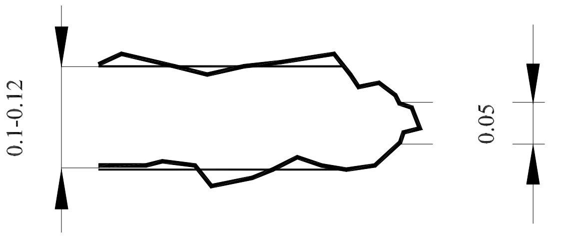

FIGURE 5. Crack tip obtained by electro-erosion

In order to evaluate weldment resistance to crack propagation J-R curves were determined by using a direct *J* integral measurement technique, as introduced in [2] and applied to welded joints [3]. Loading and strains were recorded in several loading increments during tension, Fig. 6. Strain gauges and crack mouth opening displacement (CMOD) clip gage were positioned as shown in Fig. 7.

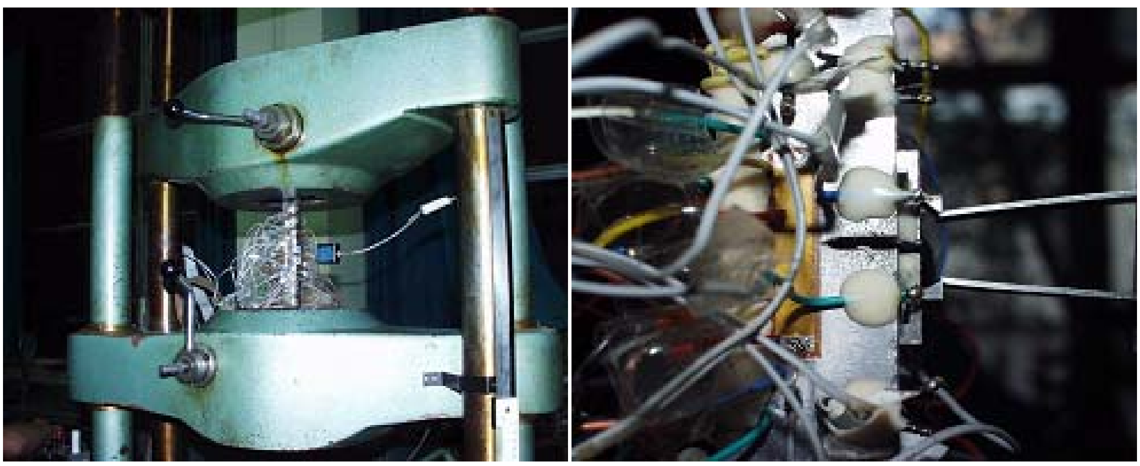

FIGURE 6. Tensile test machine with positioned specimen (left), instrumented by strain gauges and crack mouth opening displacement (CMOD) for J integral direct meausrement

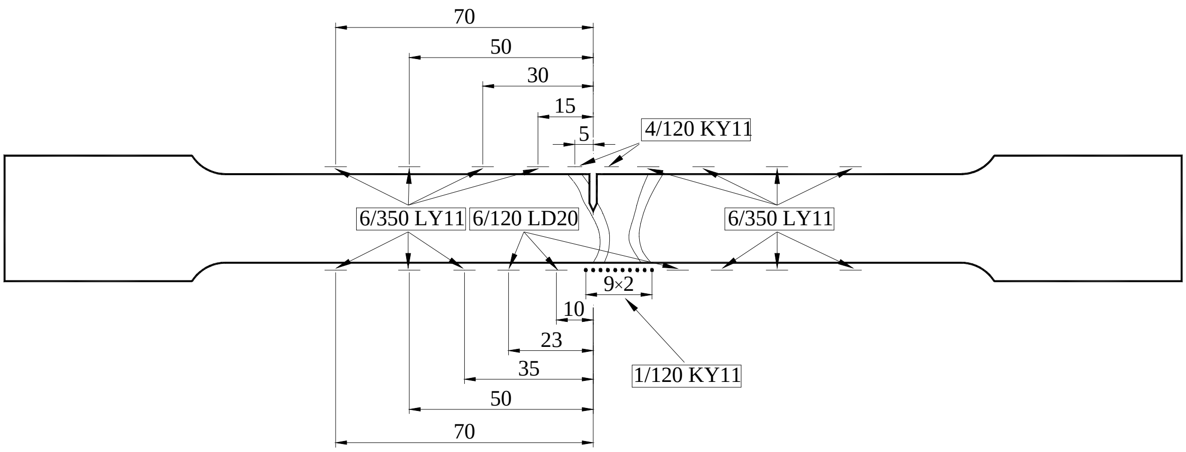

crack tip located in FGHAZ (specimen E 5-2)

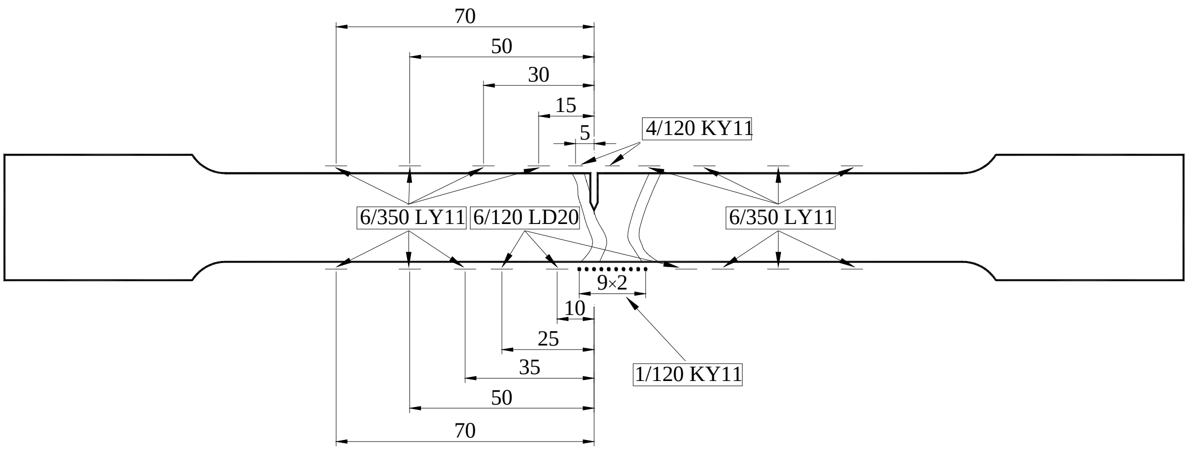

crack tip located in CGHAZ (specimen E 4-1)

FIGURE 7. Scheme for instrumentation for direct J integral measurement

The crack length was evaluated according to the following procedure:

1. The crack length after fracture was measured using standard technique (average of 9 uniformly distributed points along the crack front).
2. The slope change, indicating compliance, proportional to the crack length extension is used for the evaluation of crack extension.
3. The initial slope was assumed to be equal to the slope of linear elastic part of loading, *F*, vs. crack mouth opening displacement, CMOD, curve.

Two specimens with different crack tip position (case 1 - crack tip located in FGHAZ and case 2 - crack tip located in CGHAZ) were tested. Another pair of specimens was tested in the same way, except for the instrumentation that consisted only of CMOD clip gauges, in order to verify results.

Results in form of strain distribution are shown in Fig. 8 for case 1 and in Fig. 9 for case 2.

Using procedure defined by Read [2], the *J*-integral was evaluated. The influence of weldment mismatching was estimated as negligible, due to relatively small difference in yield strengths of WM, BM, CGHAZ and FGHAZ, as shown in [4]. Results in the form of J-R curves for both cases analyzed are presented in Fig. 10. The increase of the *J*-integral after certain amount of crack length extension, clearly recognized in diagrams, has been attributed to the consequence of mismatching and constraint effects, as explained in [1].

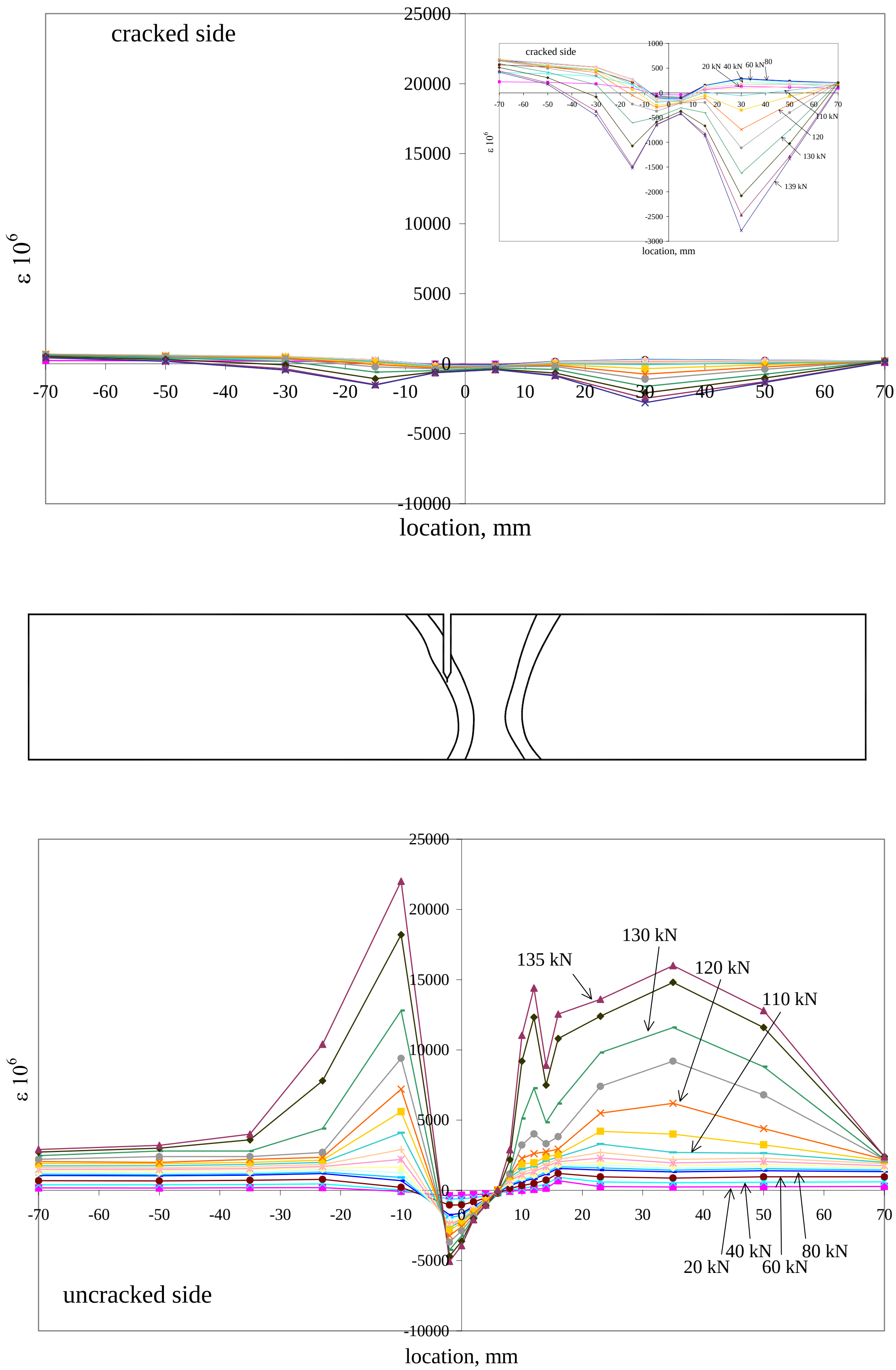

FIGURE 8. Strain distribution - specimen E 5-2 (case 1)

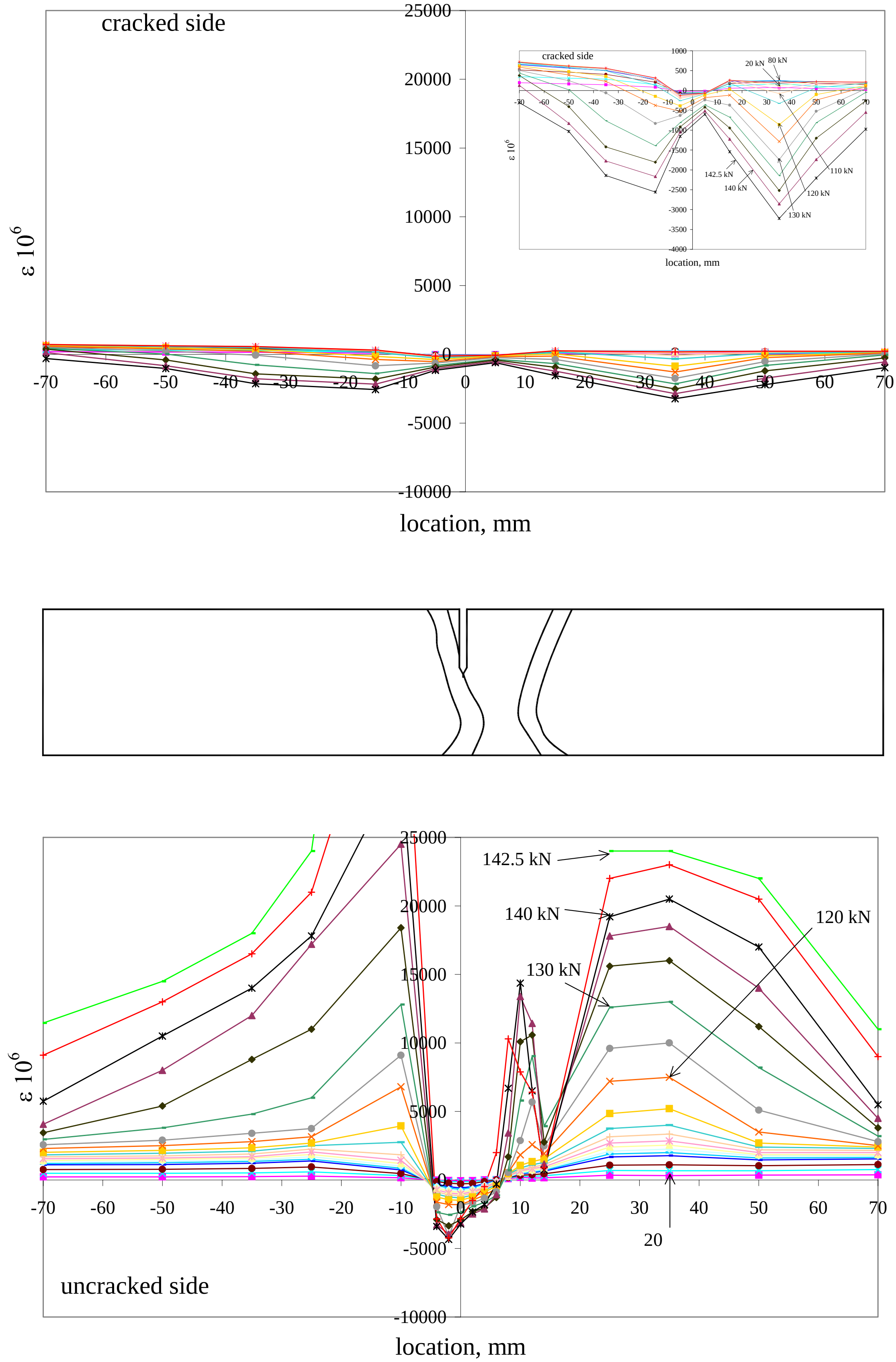

FIGURE 9. Strain distribution-specimen E 4-1 (case 2)

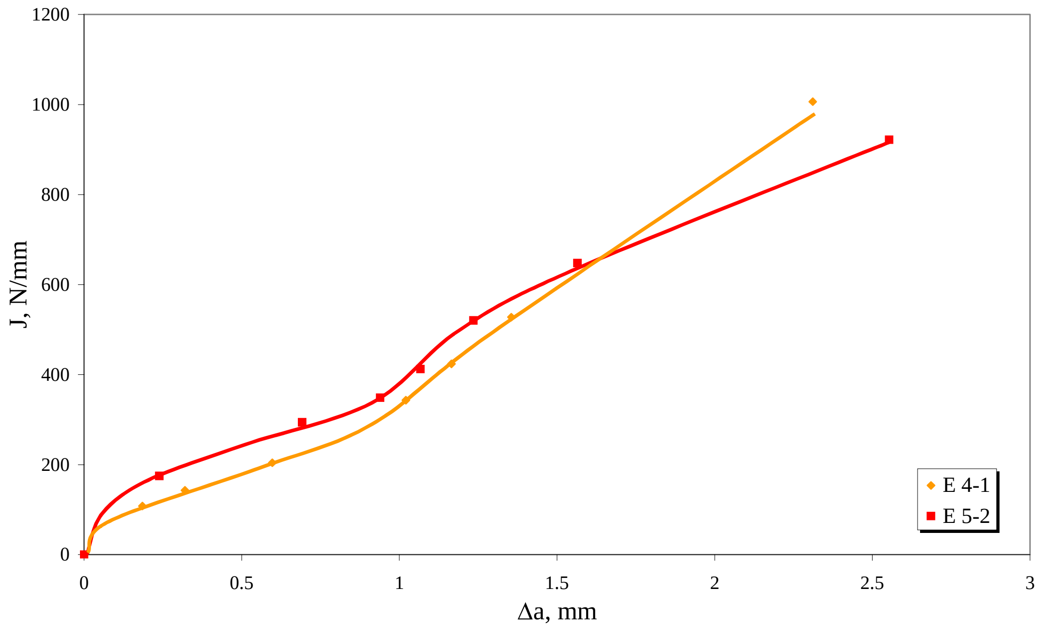

FIGURE 10. The J-R curves (E5-2 crack tip in FGHAZ, E4-1 crack tip in CGHAZ)

Assessment of the spherical tank integrity

For assessment of the spherical tank integrity crack driving (CDF) curves were compared with the material resistance to crack growth (J-Δa) curve, Fig. 11-12. The crossing point of these two curves produces the critical value of the crack driving force, which results from the criteria for ductile fracture:

$$J_{appl}(\sigma,a)=J_c \tag{1}$$

where J_{appl} is CDF, and J_c is the critical value at which the fracture failure occurs.

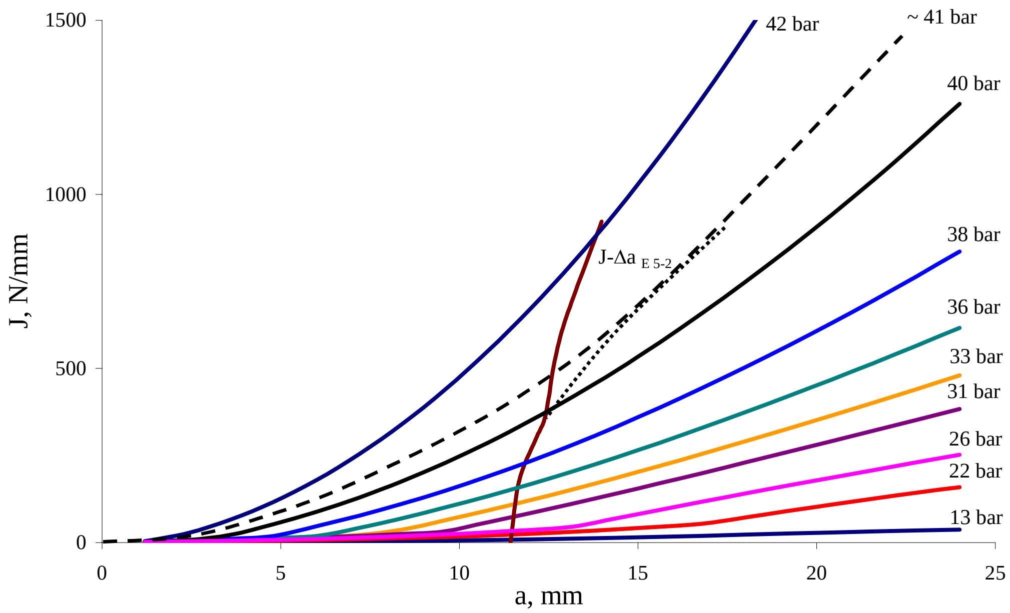

FIGURE 11. CDF versus R-curve for case 1

The CDF were obtained by the line spring method, as defined by King [5]. Here King's model is applied as the simplest analytical model which can be used when surface crack is analyzed. Since both J-Δa curves require extremely high pressures in the same figures another pair of *J*-Δ*a* curves is presented, based on an ssumption that there is no mismatching and constraint effects (dotted lines). In that case critical pressures are 41 bars and 49 bars for crack tip in FGHAZ and CGHAZ, respectively.

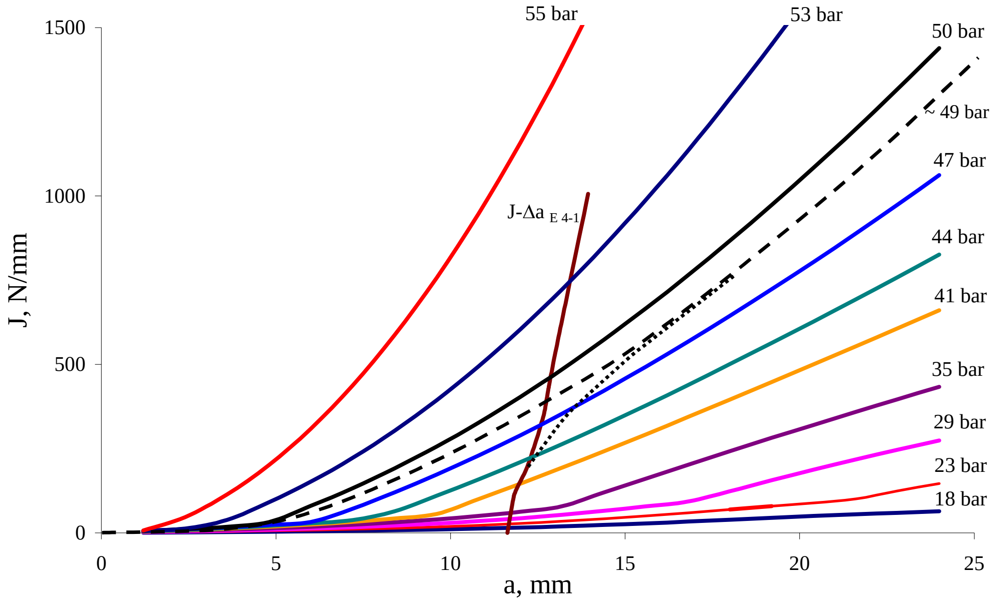

FIGURE 12. CDF versus R-curve for case 2

Conclusions

The method of *J*-integral direct measurement, although non-standardized, enables estimation of data that can not be reached by standard fracture toughness tests, and is undependable on the specimen shape and the size. Through its combination with appropriate engineering model for integrity assessment, as the King model is, a reliable analysis of the residual strength of cracked structure, such spherical pressure vessel, can be successfully performed.

The small overmatching in the welded joint has acted protective in the providing of good failure resistance. The mismatch and constraint effect, after the initial propagation of the crack in FG HAZ or CG HAZ, has changed its propagation direction toward more ductile base metal, increasing thereby the fracture resistance of a weldment.

References

1. Adziev G., *Influence of the welded joint mis-match on the integrity of the cracked welded structure*, doctoral thesis (in Macedonian), Faculty of Mechanical Engineering, Skopje, Macedonia, 2003.
2. Read, R.B., ASTM *STP 791*, ASTM, Philadelphia, USA, pp. I-444, 1983.
3. Sedmak, S, Sedmak, A., Vukomanovic, N., In *Proceedings of the Eight European Conference on Fracture*, edited by D. Firrao, Engineering Materials Advisory Services (EMAS), pp. 1596, 1990.
4. Sedmak A., *Proceedings of the Ninth International Conference on Fracture*, vol. 5, p. 2345, Pergamon Press, 1997.
5. King, R. B., *Engineering Fracture Mechanics*, vol. 18, 217-231, 1983.